C. R. Mecanique 338 (2010) 518–528

Contents lists available at ScienceDirect

Comptes Rendus Mecanique

www.sciencedirect.com

Peristaltic transport of fourth grade fluid with heat transfer and induced magnetic field

Tasawar Hayat [a,b,*], Saima Noreen [a]

[a] Department of Mathematics, Quaid-I-Azam University 45320, Islamabad 44000, Pakistan
[b] Department of Mathematics, College of Science, King Saud University, P.O. Box 2455, Riyadh 11451, Saudi Arabia

ARTICLE INFO

Article history:
Received 9 January 2010
Accepted after revision 28 June 2010
Available online 2 August 2010

Keywords:
Heat transfer
Induced magnetic field
Fourth grade fluid

ABSTRACT

We investigate the influence of an induced magnetic field on the peristaltic flow of an incompressible fourth grade fluid in a symmetric channel with heat transfer. Adopting long wavelength, low Reynolds number and small Deborah number assumptions we derive the solutions for stream function, pressure gradient, temperature, magnetic force function, induced magnetic field and current density. Qualitative agreement is demonstrated between the graphs and expected observations.

1. Introduction

Considerable attention has been directed towards the study of peristaltic transport of fluids in the physiological and engineering applications. Progressive waves have a critical role in the peristalsis. In fact such waves have been induced due to expansion and contraction of an extensible tube and propagate along the length of tube, mixing and transporting the fluid in the direction of wave propagation. This process appears in the tubular organs of the human body such as ureter, the gastro-intestinal tract etc. and peristaltic pumping has been utilized for the blood transport in the extracorporeal circulation, slurries and corrosive fluids. The transport of many fluids of physiological, pharmaceutical and industrial significance by cell separators, roller and finger pumps, heart lung machine and arthopump is because of the peristaltic mechanism. With all such motivations, several theoretical and experimental studies [1–15] have been done since the seminal work of Latham [16]. These all attempts have been presented without taking into account the effect of an induced magnetic field. Very recently, Mekheimer [17,18] and Hayat et al. [19] made critical advancement in the theory of peristaltic flows of couple stress, micropolar and third grade fluids in the presence of an induced magnetic field. On the other hand, some authors [20–26] in view of the processes of hemodialysis and oxygenation have discussed the peristaltic flows with heat transfer but in the absence of an induced magnetic field.

The present research aims to examine the simultaneous effects of heat transfer and an induced magnetic field on the peristaltic flow of fourth grade fluid in a planar channel. The solution expressions of the stream function, pressure gradient, temperature, magnetic force function, induced magnetic field and current density are derived for small Deborah number. The pumping and trapping phenomena are given proper attention. The effects of interesting parameters on the current density, temperature and an axial induced magnetic field are studied.

* Corresponding author at: Department of Mathematics, Quaid-I-Azam University 45320, Islamabad 44000, Pakistan.
E-mail address: pensy_t@yahoo.com (T. Hayat).

1631-0721/$ – see front matter
doi:10.1016/j.crme.2010.06.004

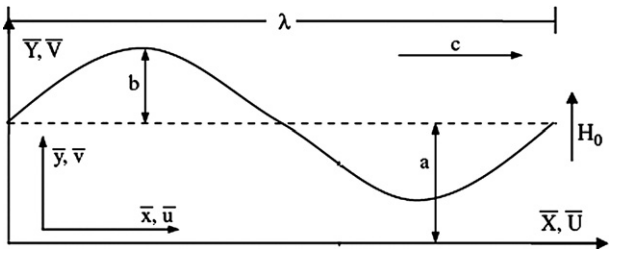

Fig. 1. Geometry of the problem.

2. Mathematical formulation

Let us consider an incompressible magnetohydrodynamic (MHD) fourth grade fluid in a planar channel of uniform thickness 2a. In Cartesian coordinate system we choose $\bar{X}$ in the direction of wave propagation and $\bar{Y}$ transverse to it. The flow description is shown in Fig. 1.

A constant magnetic field of strength H_0 acting in the transverse direction results in an induced magnetic field $\mathbf{H}(\bar{h}_{\bar{x}}(\bar{X},\bar{Y},\bar{t}),\bar{h}_{\bar{y}}(\bar{X},\bar{Y},\bar{t}),0)$. The total magnetic field is $\mathbf{H}^{+}(\bar{h}_{\bar{x}}(\bar{X},\bar{Y},\bar{t}),H_0+\bar{h}_{\bar{y}}(\bar{X},\bar{Y},\bar{t}),0)$.

The wall of the domain is represented by

$$\bar{h}(\bar{X},\bar{t}) = a + b\sin\left(\frac{2\pi}{\lambda}(\bar{X}-c\bar{t})\right) \tag{1}$$

where λ is the wavelength, a indicates the channel half width, b the wave amplitude, c the wave speed with which the infinite train of sinusoidal wave progresses along the wall in the positive $\bar{X}$ direction and $\bar{t}$ the time.

The fundamental equations governing the flow in the fixed frame are:

$$\nabla\cdot\mathbf{V} = 0 \tag{2}$$

Equation of motion

$$\begin{aligned}\rho\frac{\mathrm{d}\mathbf{V}}{\mathrm{d}t} &= \operatorname{div}\mathbf{T} + \mu_e\big(\nabla\times\mathbf{H}^{+}\big)\times\mathbf{H}^{+} + \rho g\beta_T(T-T_0)\\ &= \operatorname{div}\mathbf{T} + \mu_e\left[\big(\mathbf{H}^{+}\cdot\nabla\big)\mathbf{H}^{+} - \frac{\nabla\mathbf{H}^{+2}}{2}\right] + \rho g\beta_T(T-T_0)\end{aligned} \tag{3}$$

Energy equation

$$\rho C_p\frac{\mathrm{d}T}{\mathrm{d}t} = \kappa\nabla^2 T + Q_0 \tag{4}$$

Induction equation

$$\frac{\mathrm{d}\mathbf{H}^{+}}{\mathrm{d}\bar{t}} = \nabla\times\big(\mathbf{V}\times\mathbf{H}^{+}\big) + \frac{1}{\varsigma}\nabla^2\mathbf{H}^{+} \tag{5}$$

In above equations $\varsigma = \sigma\mu_e$ is the magnetic diffusivity, C_p the specific heat, T the temperature, Q_0 the constant of heat conduction and absorption and κ the thermal conductivity.

The Cauchy stress tensor $\bar{\mathbf{T}}$ (with pressure p, identity tensor $\bar{\mathbf{I}}$ and an extra stress tensor $\bar{\mathbf{S}}$) is:

$$\bar{\mathbf{T}} = -p\bar{\mathbf{I}} + \bar{\mathbf{S}} \tag{6}$$

$$\begin{aligned}\bar{\mathbf{S}} &= \mu\bar{\mathbf{A}}_1 + \alpha_1\bar{\mathbf{A}}_2 + \alpha_2\bar{\mathbf{A}}_1^2 + \beta_1'\bar{\mathbf{A}}_3 + \beta_2'(\bar{\mathbf{A}}_2\bar{\mathbf{A}}_1 + \bar{\mathbf{A}}_1\bar{\mathbf{A}}_2) + \beta_3'(\operatorname{tr}\bar{\mathbf{A}}_2)\bar{\mathbf{A}}_1 + \gamma_1\bar{\mathbf{A}}_4\\ &\quad + \gamma_2(\bar{\mathbf{A}}_3\bar{\mathbf{A}}_1 + \bar{\mathbf{A}}_1\bar{\mathbf{A}}_3) + \gamma_3\bar{\mathbf{A}}_2^2 + \gamma_4\big(\bar{\mathbf{A}}_2\bar{\mathbf{A}}_1^2 + \bar{\mathbf{A}}_1^2\bar{\mathbf{A}}_2\big) + \gamma_5(\operatorname{tr}\bar{\mathbf{A}}_2)\bar{\mathbf{A}}_2\\ &\quad + \gamma_6(\operatorname{tr}\bar{\mathbf{A}}_2)\bar{\mathbf{A}}_1^2 + \big\{\gamma_7\operatorname{tr}\bar{\mathbf{A}}_3 + \gamma_8\operatorname{tr}(\bar{\mathbf{A}}_2\bar{\mathbf{A}}_1)\big\}\bar{\mathbf{A}}_1\end{aligned} \tag{7}$$

$$\bar{\mathbf{A}}_n = \frac{\mathrm{d}\bar{\mathbf{A}}_n}{\mathrm{d}\bar{t}} + \bar{\mathbf{A}}_{n-1}(\operatorname{grad}\bar{\mathbf{V}}) + (\operatorname{grad}\bar{\mathbf{V}})^T\bar{\mathbf{A}}_{n-1},\quad n>1 \tag{8}$$

$$\bar{\mathbf{A}}_1 = (\operatorname{grad}\bar{\mathbf{V}}) + (\operatorname{grad}\bar{\mathbf{V}})^T \tag{9}$$

where α_i $(i=1,2)$, β_j' $(j=1\text{–}3)$ and γ_l $(l=1\text{–}8)$ are the material constants, $\bar{\mathbf{A}}_n$ the Rivilin–Ericksen tensors $\mathrm{d}/\mathrm{d}\bar{t}$ the material derivative, μ the viscosity, tr the trace, T in the superscript is the matrix transpose and the velocity $\bar{\mathbf{V}}$ for two-dimensional flow is

$$\bar{\mathbf{V}} = \left[\bar{U}(\bar{X},\bar{Y},\bar{t}), \bar{V}(\bar{X},\bar{Y},\bar{t}), 0\right] \tag{10}$$

The Maxwell's relations in the absence of displacement current are

$$\nabla\cdot\mathbf{E} = 0, \qquad \nabla\cdot\mathbf{H} = 0 \tag{11}$$

$$\nabla\times\mathbf{E} = -\mu_e\frac{\partial\mathbf{H}}{\partial t}, \qquad \nabla\times\mathbf{H} = \mathbf{J} \tag{12}$$

and

$$\mathbf{J} = \sigma\left(\mathbf{E} + \mu_e(\mathbf{V}\times\mathbf{H})\right) \tag{13}$$

Here $\mathbf{J}$, μ_e, σ, $\mathbf{E}$ and $\mathbf{H}$ denote the electric current density, the magnetic permeability, the electrical conductivity, the electric field and the magnetic field respectively.

It is noticed that the unsteady flow in the fixed frame $(\bar{X},\bar{Y})$ appears steady in the wave frame $(\bar{x},\bar{y})$ by the following relations:

$$\begin{aligned}&\bar{x} = \bar{X} - c\bar{t}, \qquad \bar{y} = \bar{Y}\\ &\bar{u}(\bar{x},\bar{y}) = \bar{U} - c, \qquad \bar{v}(\bar{x},\bar{y}) = \bar{V}\end{aligned} \tag{14}$$

in which $(\bar{U},\bar{V})$ and $(\bar{u},\bar{v})$ are the velocity components in the fixed and wave frames respectively.

In the wave frame the resulting equations are

$$\frac{\partial\bar{u}}{\partial\bar{x}} + \frac{\partial\bar{v}}{\partial\bar{y}} = 0 \tag{15}$$

$$\rho\left(\bar{u}\frac{\partial}{\partial\bar{x}} + \bar{v}\frac{\partial}{\partial\bar{y}}\right)\bar{u} + \frac{\partial\bar{p}}{\partial\bar{x}} = \frac{\partial\bar{S}_{xx}}{\partial\bar{x}} + \frac{\partial\bar{S}_{xy}}{\partial\bar{y}} - \frac{\mu_e}{2}\left(\frac{\partial H^{+^2}}{\partial\bar{x}}\right) + \mu_e\left(\bar{h}_{\bar{x}}\frac{\partial\bar{h}_x}{\partial\bar{x}} + \bar{h}_{\bar{y}}\frac{\partial\bar{h}_x}{\partial\bar{y}} + H_0\frac{\partial\bar{h}_x}{\partial\bar{y}}\right) + \rho g\beta_T(T - T_0) \tag{16}$$

$$\rho\left(\bar{u}\frac{\partial}{\partial\bar{x}} + \bar{v}\frac{\partial}{\partial\bar{y}}\right)\bar{v} + \frac{\partial\bar{p}}{\partial\bar{y}} = \frac{\partial\bar{S}_{yx}}{\partial\bar{x}} + \frac{\partial\bar{S}_{yy}}{\partial\bar{y}} - \frac{\mu_e}{2}\left(\frac{\partial H^{+^2}}{\partial\bar{y}}\right) + \mu_e\left(\bar{h}_{\bar{x}}\frac{\partial\bar{h}_{\bar{y}}}{\partial\bar{x}} + \bar{h}_{\bar{y}}\frac{\partial\bar{h}_{\bar{y}}}{\partial\bar{y}} + H_0\frac{\partial\bar{h}_{\bar{y}}}{\partial\bar{y}}\right) \tag{17}$$

$$\rho C_p\left[\bar{u}\frac{\partial}{\partial\bar{x}} + \bar{v}\frac{\partial}{\partial\bar{y}}\right]\bar{T} = \kappa\left[\frac{\partial^2\bar{T}}{\partial\bar{x}^2} + \frac{\partial^2\bar{T}}{\partial\bar{y}^2}\right] + Q_0 \tag{18}$$

We introduce the following non-dimensional quantities

$$\begin{aligned}&x = \frac{\bar{x}}{\lambda}, \quad y = \frac{\bar{y}}{a}, \quad t = \frac{c\bar{t}}{\lambda}, \quad p = \frac{a^2\bar{p}}{c\lambda\mu}, \quad M^2 = Re\,S^2R_m, \quad \lambda_i = \frac{\alpha_i c}{\mu a} \quad (i = 1,2)\\ &\delta = \frac{a}{\lambda}, \quad S_{ij} = \frac{a\bar{S}_{ij}}{\mu c} \quad (\text{for } i,j = 1,2,3), \quad u = \frac{\bar{u}}{c}, \quad v = \frac{\bar{v}}{c}\\ &Re = \frac{ca\rho}{\mu}, \quad R_m = \sigma\mu_e ac, \quad S = \frac{H_0}{c}\sqrt{\frac{\mu_e}{\rho}}, \quad \phi = \frac{\bar{\phi}}{H_0 a}, \quad \eta_k = \frac{\gamma_k c^3}{\mu a^3} \quad (k = 1\text{–}8)\\ &\bar{h}_{\bar{x}} = \bar{\phi}_{\bar{y}}, \quad \bar{h}_{\bar{y}} = -\bar{\phi}_{\bar{x}}, \quad p_m = p + \frac{1}{2}Re\,\delta\frac{\mu_e(H^+)^2}{\rho c^2}, \quad E = \frac{-\bar{E}}{cH_0\mu_e}\\ &Pr = \frac{\mu C_p}{\kappa}, \quad \gamma = \frac{\bar{T} - T_0}{T_0}, \quad Gr = \frac{\beta_T g T_0}{c\nu}\\ &\beta_1 = \frac{Q_0 a_1^2}{\kappa T_0}, \quad \xi_j = \frac{\beta_j' c^2}{\mu a} \quad (j = 1,2,3)\end{aligned} \tag{19}$$

where Pr, δ, Re, R_m, S and M are the Prandtl, wave, Reynolds, magnetic Reynolds, Strommer's and Hartman numbers respectively. Here p_m is the total pressure which is sum of ordinary and magnetic pressures, E is the electric field strength, β_1 is the heat source/sink parameter, γ is the temperature and ϕ is the magnetic force function. Moreover T_0 is the temperature at $y = h$.

The non-dimensional configuration of the peristaltic wave can be represented by

$$h = \frac{\bar{h}}{a} = 1 + \alpha\sin(2\pi x) \tag{20}$$

in which the amplitude ratio α is equal to b/a.

Using

$$u=\frac{\partial\Psi}{\partial y},\qquad v=-\delta\frac{\partial\Psi}{\partial x},\qquad h_x=\frac{\partial\phi}{\partial y},\qquad h_y=-\delta\frac{\partial\phi}{\partial x} \tag{21}$$

Eq. (2) is automatically satisfied and Eqs. (3)–(18) can be arranged as

$$Re\,\delta\left(\frac{\partial\Psi}{\partial y}\frac{\partial}{\partial x}-\frac{\partial\Psi}{\partial x}\frac{\partial}{\partial y}\right)\frac{\partial\Psi}{\partial y}+\frac{\partial p_m}{\partial x}=\delta\frac{\partial S_{xx}}{\partial x}+\frac{\partial S_{xy}}{\partial y}+\delta\,Re\,S^2\left(\frac{\partial\phi}{\partial y}\frac{\partial}{\partial x}-\frac{\partial\phi}{\partial x}\frac{\partial}{\partial y}\right)\frac{\partial\phi}{\partial y}+Re\,S^2\frac{\partial^2\phi}{\partial y^2}+Gr\,\gamma \tag{22}$$

$$-Re\,\delta^2\left(\frac{\partial\Psi}{\partial y}\frac{\partial}{\partial x}-\frac{\partial\Psi}{\partial x}\frac{\partial}{\partial y}\right)\frac{\partial\Psi}{\partial x}+\frac{\partial p_m}{\partial y}=\delta\left(\delta\frac{\partial S_{yx}}{\partial x}+\frac{\partial S_{yy}}{\partial y}\right)-\delta^3\,Re\,S^2\left(\frac{\partial\phi}{\partial y}\frac{\partial}{\partial x}-\frac{\partial\phi}{\partial x}\frac{\partial}{\partial y}\right)\frac{\partial\phi}{\partial x}-Re\,\delta^2S^2\frac{\partial^2\phi}{\partial x\partial y} \tag{23}$$

$$\delta\,Pr\,Re\left[\frac{\partial\Psi}{\partial y}\frac{\partial\gamma}{\partial x}-\frac{\partial\Psi}{\partial x}\frac{\partial\gamma}{\partial y}\right]=\delta^2\frac{\partial^2\gamma}{\partial x^2}+\frac{\partial^2\gamma}{\partial y^2}+\beta_1 \tag{24}$$

$$E=\frac{\partial\Psi}{\partial y}-\delta\left(\frac{\partial\Psi}{\partial y}\frac{\partial\phi}{\partial x}-\frac{\partial\Psi}{\partial x}\frac{\partial\phi}{\partial y}\right)+\frac{1}{R_m}\left(\delta^2\frac{\partial^2}{\partial x^2}+\frac{\partial^2}{\partial y^2}\right)\phi \tag{25}$$

Note that the values of S_{xx}, S_{xy} and S_{yy} can be computed by employing Eqs. (7)–(10) and (21). Hence Eqs. (22)–(25) under long wavelength and low Reynolds number approximations takes the form

$$\frac{\partial p}{\partial x}=\frac{\partial S_{xy}}{\partial y}+Re\,S^2\frac{\partial^2\phi}{\partial y^2}+Gr\,\gamma \tag{26}$$

$$\frac{\partial p}{\partial y}=0 \tag{27}$$

$$\frac{\partial^2\gamma}{\partial y^2}+\beta_1=0 \tag{28}$$

$$E=\frac{\partial\Psi}{\partial y}+\frac{1}{R_m}\frac{\partial^2\phi}{\partial y^2} \tag{29}$$

The dimensionless boundary conditions are

$$\begin{aligned}&\Psi=0,\qquad \frac{\partial^2\Psi}{\partial y^2}=0,\qquad \frac{\partial\phi}{\partial y}=0,\quad \text{at } y=0\\ &\Psi=F,\qquad \frac{\partial\Psi}{\partial y}=-1,\qquad \phi=0,\quad \text{at } y=h\\ &\frac{\partial\gamma}{\partial y}=0,\quad \text{at } y=0\\ &\gamma=0,\quad \text{at } y=h\end{aligned} \tag{30}$$

where F is the dimensionless time mean flow rate in the wave frame. It is related to dimensionless time mean flow rate θ in the laboratory frame through the expression $\theta=F+1$ in which

$$F=\int_0^h\frac{\partial\Psi}{\partial y}\,\mathrm{d}y \tag{31}$$

and through Eq. (27) $p\neq p(y)$. The modified form of Eq. (26) is given by

$$\frac{\partial p}{\partial x}=\frac{\partial}{\partial y}\left[\Psi_{yy}\left\{1+2\Gamma\left(\frac{\partial^2\Psi}{\partial y^2}\right)^2\right\}\right]+M^2\left(E-\frac{\partial\Psi}{\partial y}\right)+Gr\,\gamma \tag{32}$$

where $\Gamma=\xi_2+\xi_3$ is the Deborah number.

By Eqs. (27) and (32) we have

$$\frac{\partial^4\Psi}{\partial y^4}+2\Gamma\frac{\partial^2}{\partial y^2}\left(\frac{\partial^2\Psi}{\partial y^2}\right)^3-M^2\frac{\partial^2\Psi}{\partial y^2}+Gr\frac{\partial\gamma}{\partial y}=0 \tag{33}$$

3. Perturbation solution

Looking for a perturbation solution we first write

$$\Psi = \Psi_0 + \Gamma\Psi_1 + O(\Gamma)^2 \tag{34}$$
$$F = F_0 + \Gamma F_1 + O(\Gamma)^2 \tag{35}$$
$$p = p_0 + \Gamma p_1 + O(\Gamma)^2 \tag{36}$$
$$\phi = \phi_0 + \Gamma\phi_1 + O(\Gamma)^2 \tag{37}$$
$$\gamma = \gamma_0 + \Gamma\gamma_1 + O(\Gamma)^2 \tag{38}$$

and then use in Eqs. (29) and (33). After doing this we get the equations of the next subsection.

3.1. Zeroth order system

$$\frac{\partial^4\Psi_0}{\partial y^4} - M^2\frac{\partial^2\Psi_0}{\partial y^2} + Gr\frac{\partial\gamma_0}{\partial y} = 0$$
$$\frac{\partial p_0}{\partial x} = \frac{\partial^3\Psi_0}{\partial y^3} + M^2\left(E - \frac{\partial\psi_0}{\partial y}\right) + Gr\,\gamma_0$$
$$\frac{\partial^2\phi_0}{\partial y^2} = R_m\left(E - \frac{\partial\psi_0}{\partial y}\right)$$
$$\frac{\partial^2\gamma_0}{\partial y^2} + \beta_1 = 0$$

$$\Psi_0 = 0, \qquad \frac{\partial^2\Psi_0}{\partial y^2} = 0, \qquad \frac{\partial\phi_0}{\partial y} = 0, \qquad \frac{\partial\gamma_0}{\partial y} = 0, \quad \text{at } y = 0$$
$$\Psi_0 = F_0, \qquad \frac{\partial\Psi_0}{\partial y} = -1, \qquad \phi_0 = 0, \qquad \gamma_0 = 0, \quad \text{at } y = h \tag{39}$$

3.2. First order system

$$\frac{\partial^4\Psi_1}{\partial y^4} - M^2\frac{\partial^2\Psi_1}{\partial y^2} + 2\frac{\partial^2}{\partial y^2}\left(\frac{\partial^2\psi_0}{\partial y^2}\right)^3 + Gr\frac{\partial\gamma_1}{\partial y} = 0$$
$$\frac{\partial p_1}{\partial x} = \frac{\partial^3\Psi_1}{\partial y^3} + 2\frac{\partial}{\partial y}\left(\frac{\partial^2\Psi_0}{\partial y^2}\right)^3 - M^2\frac{\partial\psi_1}{\partial y} + Gr\,\gamma_1$$
$$\frac{\partial^2\phi_1}{\partial y^2} = -R_m\frac{\partial\psi_1}{\partial y}$$
$$\frac{\partial^2\gamma_1}{\partial y^2} = 0$$

$$\Psi_1 = 0, \qquad \frac{\partial^2\Psi_1}{\partial y^2} = 0, \qquad \frac{\partial\phi_1}{\partial y} = 0, \qquad \frac{\partial\gamma_1}{\partial y} = 0, \quad \text{at } y = 0$$
$$\Psi_1 = F_1, \qquad \frac{\partial\Psi_1}{\partial y} = 0, \qquad \phi_1 = 0, \qquad \gamma_1 = 0, \quad \text{at } y = h \tag{40}$$

Solving the resulting zeroth and first order systems and then invoking

$$F_0 = F - \Gamma F_1 \tag{41}$$

we obtain the following expressions

$$\psi = \frac{B_0}{6M^2}\big(\cosh(My) - \sinh(My)\big)C_1(y) + \Gamma\left[\frac{B_0^4}{108M^8}\big(\cosh(3My) - \sinh(3My)\big)\sum_{i=2}^{17}C_i(y)\right] \tag{42}$$

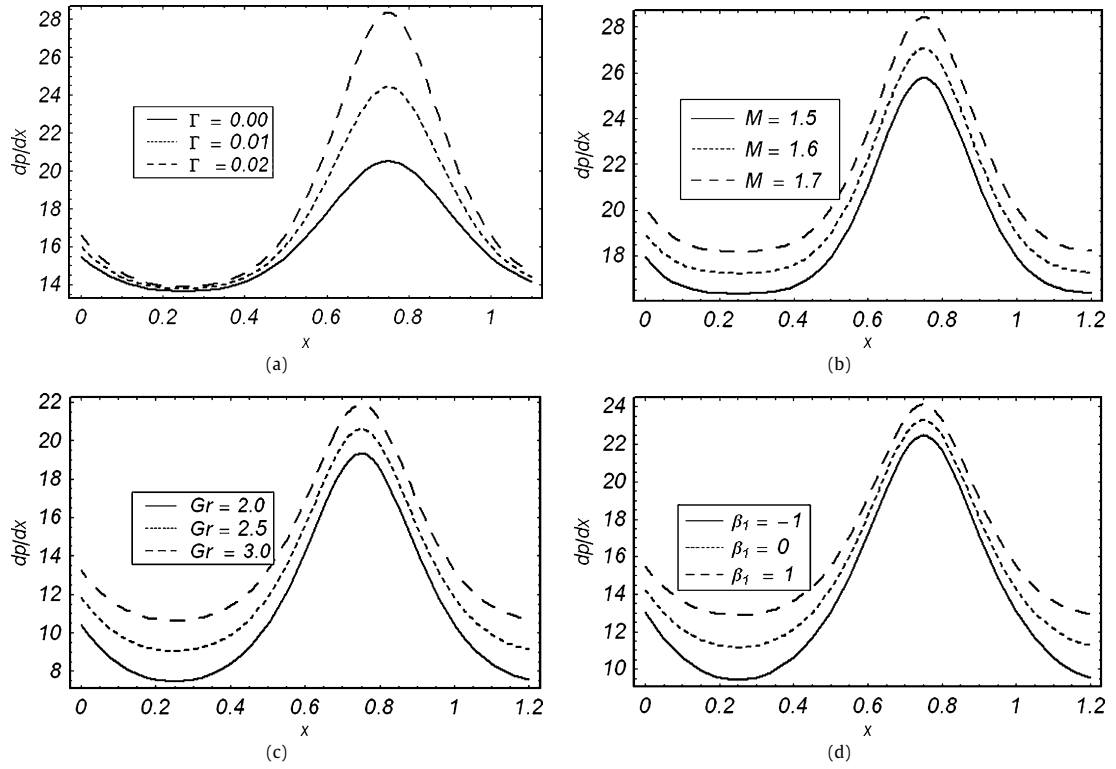

Fig. 2. The pressure gradient $\mathrm{d}p/\mathrm{d}x$ versus x for $\beta_1 = 1$, $\alpha = 0.2$, $M = 1.5$, $Gr = 5$, $E = 0$ and $\theta = -1.1$ (a); $\beta_1 = 1$, $\alpha = 0.2$, $\Gamma = 0.01$, $Gr = 3$, $E = 1$ and $\theta = -1.1$ (b); $\beta_1 = 1$, $\alpha = 0.2$, $\Gamma = 0.01$, $M = 1.5$, $E = 0$ and $\theta = -1.1$ (c); $\alpha = 0.2$, $Gr = 3$, $\Gamma = 0.01$, $M = 1.5$, $E = 1$ and $\theta = -1.1$ (d).

$$\frac{\mathrm{d}p}{\mathrm{d}x} = \frac{B_0^4}{3M^2}\big(\cosh(3My) - \sinh(3My)\big)\big(L_1(y) + L_2(y)\big) + \Gamma\left[-\frac{B_0^4}{54M^8}\big(\cosh(3My) - \sinh(3My)\big)\sum_{j=3}^{5} L_j(y)\right] \tag{43}$$

$$\phi = \frac{B_0 R_m}{2M}\big(\cosh(My) - \sinh(My)\big)B_1(y) + \Gamma\left[\frac{R_m B_0^4}{324M^9}\big(\cosh(3My) - \sinh(3My)\big)\sum_{k=2}^{15} B_k(y)\right] \tag{44}$$

$$\gamma = \frac{1}{2}\beta_1\big(h^2 - y^2\big) \tag{45}$$

where the values of the involved L_j $(j = 1\text{–}5)$, B_k $(k = 0\text{–}15)$ and C_i $(i = 1\text{–}17)$ are given in Supplementary material.

The dimensionless axial induced magnetic field h_x, current density J_z and pressure rise ΔP_λ are defined as

$$h_x = \frac{\partial \phi}{\partial y} \tag{46}$$

$$J_z = -\frac{\partial h_x}{\partial y} \tag{47}$$

$$\Delta P_\lambda = \int_0^1 \left(\frac{\mathrm{d}p}{\mathrm{d}x}\right)_{y=0} \mathrm{d}x \tag{48}$$

4. Graphical results and discussion

The purpose of this section is to study the influences of various parameters (i.e. material parameter Γ, Grashof number Gr, sink/source parameter β_1, amplitude ratio α, Hartman number M and magnetic Reynolds number R_m) on the temperature γ, current density J_z, axial induced magnetic field h_x, pressure gradient $\mathrm{d}p/\mathrm{d}x$, pressure rise ΔP_λ and axial velocity u. Figs. 1–6 illustrate the effects of such variations.

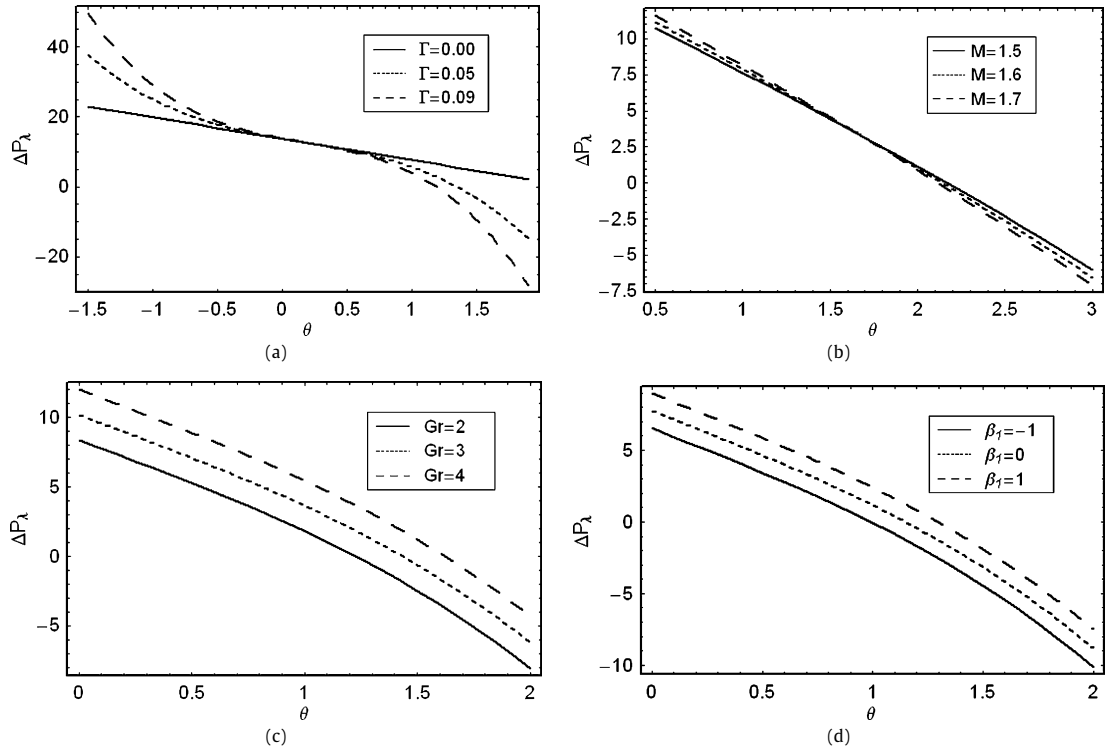

Fig. 3. The pressure rise ΔP_λ versus flow rate θ for $\beta_1 = 2$, $\alpha = 0.2$, $M = 1.5$, $Gr = 5$ and $E = 1$ (a); $\beta_1 = 2$, $\alpha = 0.2$, $\Gamma = 0.01$, $Gr = 5$ and $E = 1$ (b); $\beta_1 = 2$, $\alpha = 0.2$, $\Gamma = 0.01$, $M = 1.5$ and $E = 1$ (c); $Gr = 3$, $\alpha = 0.2$, $\Gamma = 0.01$, $Gr = 5$ and $E = 1$ (d).

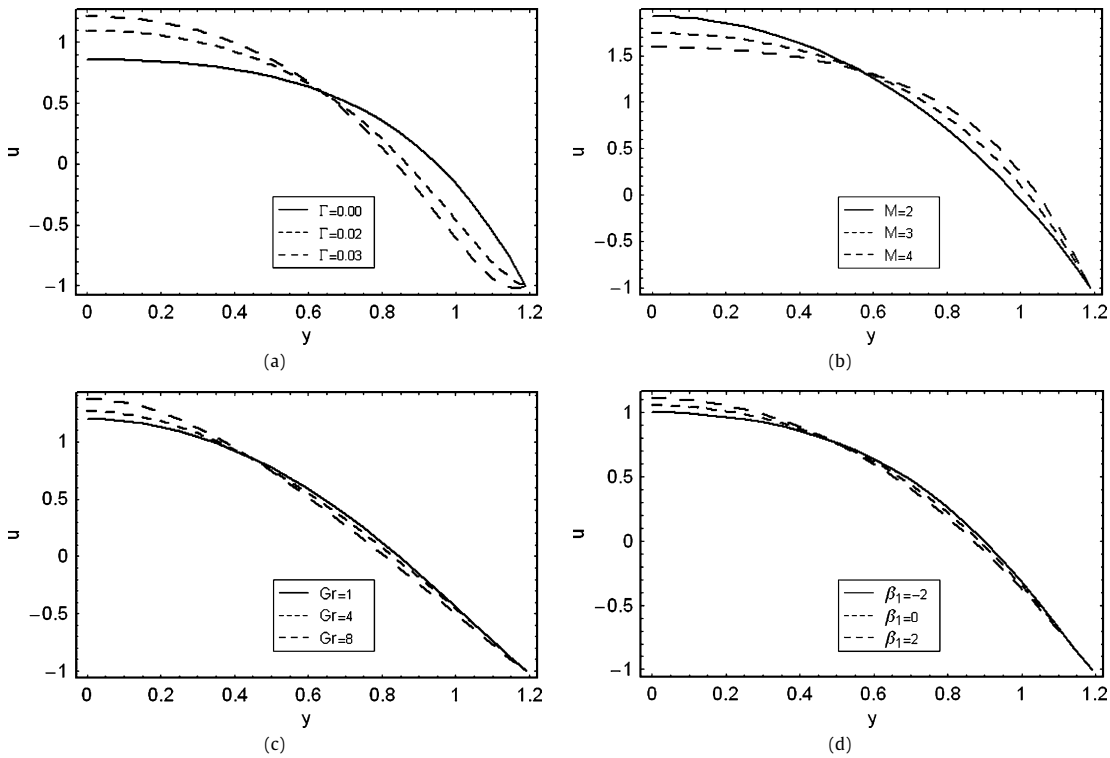

Fig. 4. The axial velocity u for $x = 0.2$, $Gr = 3$, $\alpha = 0.2$, $\beta_1 = -3$, $\theta = 1.5$, $Gr = 5$ and $M = 2$ (a); $x = 0.2$, $Gr = 3$, $\Gamma = 0.01$, $\beta_1 = 3$, $\theta = 2.2$, $Gr = 3$ and $\alpha = 0.2$ (b); $x = 0.2$, $M = 1.5$, $\Gamma = 0.02$, $\beta_1 = 3$, $\theta = 1.5$ and $\alpha = 0.2$ (c); $x = 0.2$, $M = 2$, $\Gamma = 0.01$, $\beta_1 = 3$, $\theta = 1.5$ and $\alpha = 0.2$ (d).

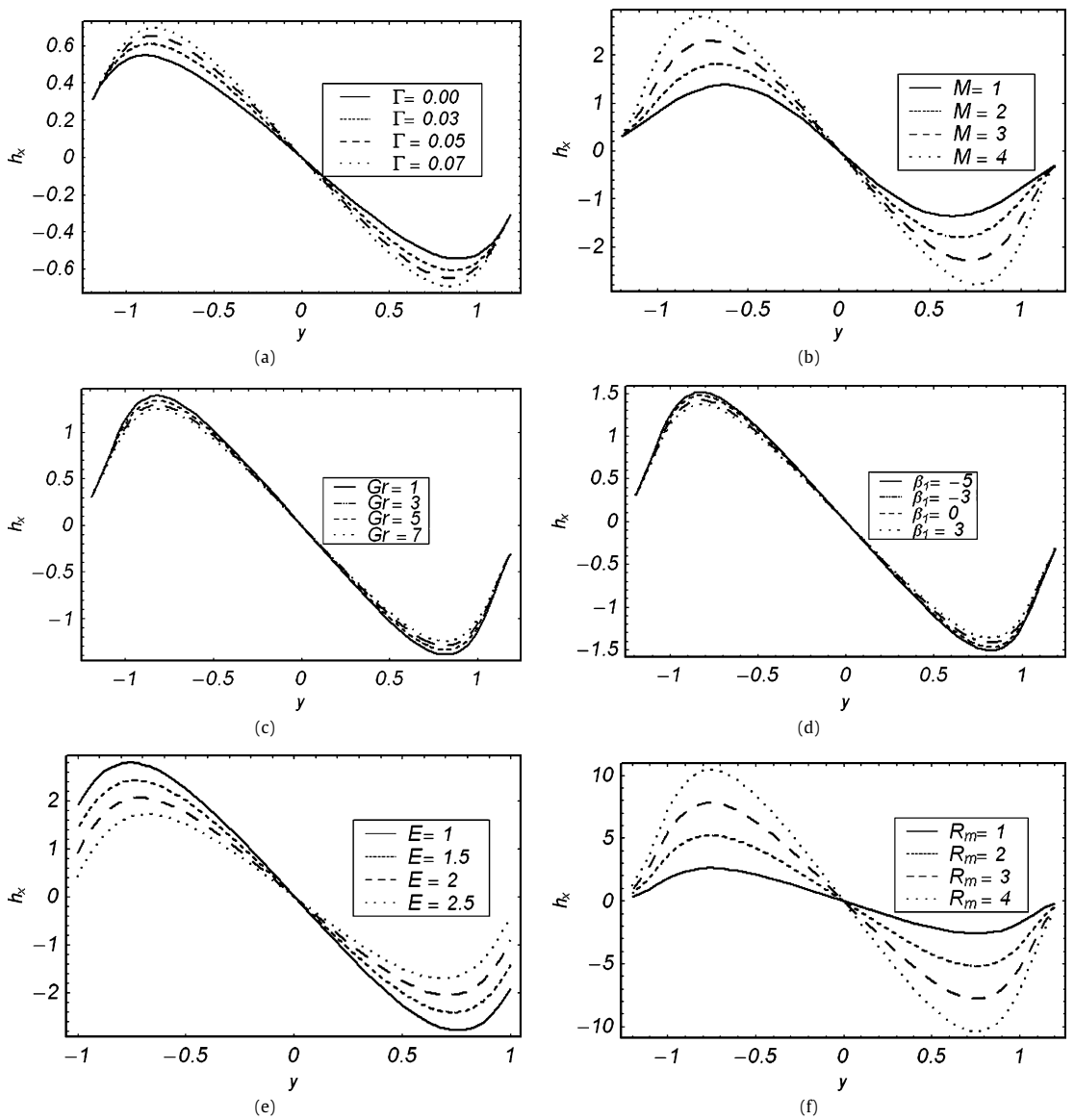

Fig. 5. The axial induced magnetic field h_x versus y for $M = 4.5$, $\beta_1 = 3$, $\theta = 2.5$, $x = 0.2$, $\alpha = 0.2$, $R_m = 1$, $Gr = 3$ and $E = 1$ (a); $\Gamma = 0.1$, $\beta_1 = 3$, $\theta = 2.5$, $x = 0.2$, $\alpha = 0.2$, $R_m = 1$, $Gr = 3$ and $E = 1$ (b); $\Gamma = 0.03$, $M = 5.5$, $\beta_1 = 3$, $\theta = 2.5$, $x = 0.2$, $\alpha = 0.2$, $R_m = 1$ and $E = 1$ (c); $M = 5.5$, $Gr = 2$, $\theta = 2.5$, $x = 0.2$, $\alpha = 0.2$, $R_m = 1$, $\Gamma = 0.03$ and $E = 1$ (d); $M = 4.5$, $Gr = 3$, $\theta = 2.5$, $x = 0.2$, $\alpha = 0.2$, $R_m = 1$, $\Gamma = 0.1$ and $\beta_1 = 3$ (e); $M = 4.5$, $Gr = 3$, $\theta = 2.5$, $x = 0.2$, $\alpha = 0.2$, $E = 1$, $\Gamma = 0.1$ and $\beta_1 = 3$ (f).

4.1. Pumping characteristics

Fig. 2 plots the dimensionless pressure gradient $\mathrm{d}p/\mathrm{d}x$ with x. Through Figs. 2(a)–2(d) we can see that $\mathrm{d}p/\mathrm{d}x$ is an increasing function of Γ, M, Gr and β_1 respectively. In the wider part of channel $x \in [0, 0.5]$ and $x \in [1, 1.2]$ the pressure gradient is relatively small i.e. flow can easily pass without the imposition of large pressure gradient. In the narrow part of channel $x \in [0.5, 1]$ much larger pressure gradient is required to maintain the flux to pass through it.

Pumping action is due to the dynamic pressure exerted by the walls on the fluid trapped between the contraction region. Pumping against pressure rise is plotted in Fig. 3. The pressure rise ΔP_λ is sketched against the flow rate θ (in waveframe). Pumping action divides the region into four sections: pumping region ($\Delta p_\lambda > 0,\ \theta > 0$), augmented pumping ($\Delta p_\lambda < 0,\ \theta > 0$), retrograde pumping ($\Delta p_\lambda > 0,\ \theta < 0$) and free pumping $\Delta p_\lambda = 0$. It is seen in Fig. 3(a) that pumping performance is better for $\Delta p_\lambda > 20$ and for certain values of flow rate the pumping curves coincide showing that there is no difference between the Newtonian and fourth grade fluids. For appropriate values of $\Delta p_\lambda < 10$, the pumping rate decreases by increasing the values of Γ. For $\Gamma = 0$ there is linear relationship between pressure rise and flow rate. However

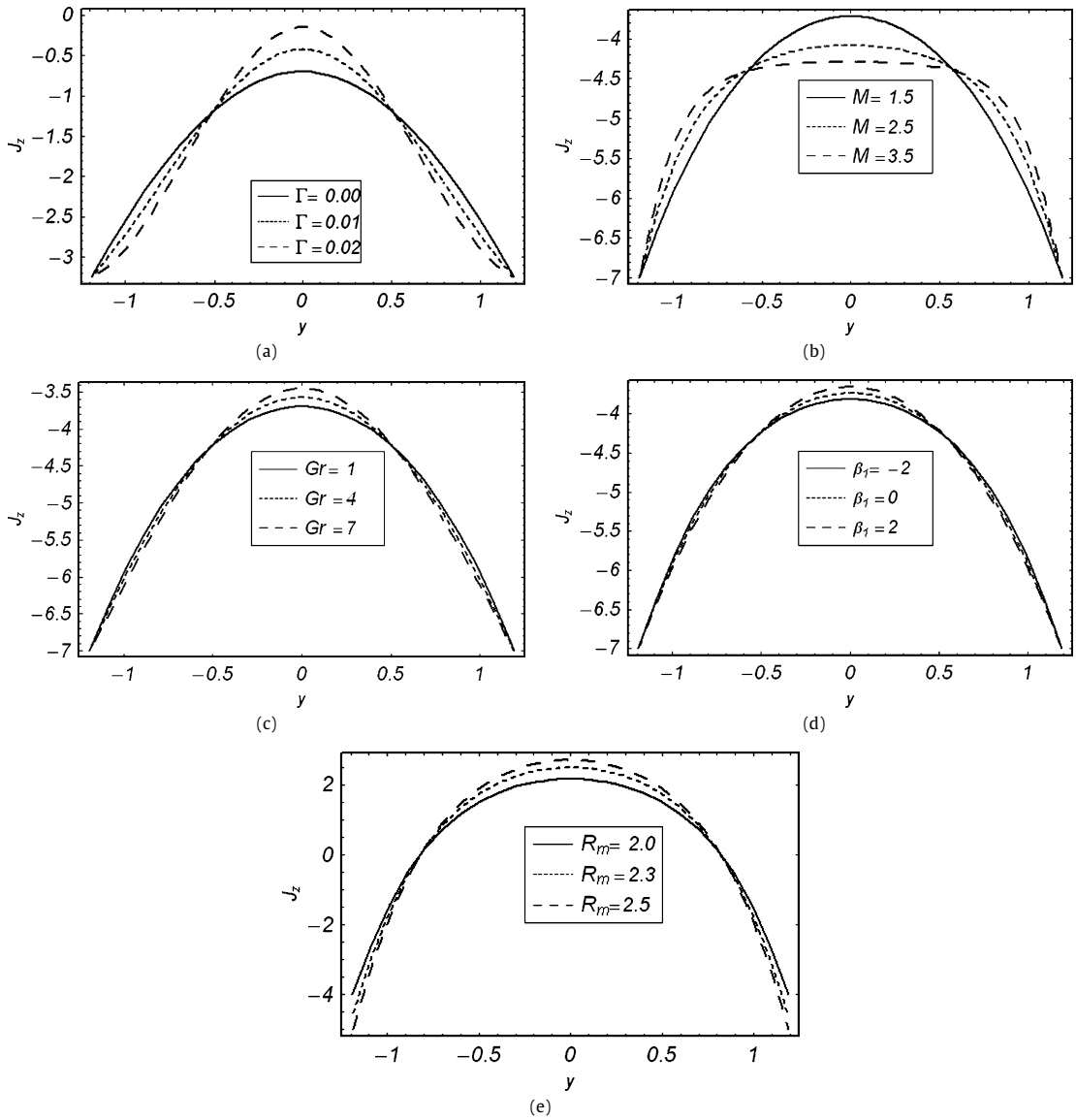

Fig. 6. Current density J_z versus y for $R_m = 0.5$, $\beta_1 = 3$, $M = 1.2$, $Gr = 5$, $\theta = 3.8$, $x = 0.2$, $\alpha = 0.2$ and $E = 5.5$ (a); $R_m = 1$, $\alpha = 0.2$, $\Gamma = 0.001$, $\beta_1 = 3$, $x = 0.2$, $E = 6$ and $\theta = 2.5$ (b); $M = 1.5$, $R_m = 1$, $\alpha = 0.2$, $\Gamma = 0.001$, $\beta_1 = 3$, $x = 0.2$, $E = 6$ and $\theta = 2.5$ (c); $M = 1.5$, $R_m = 1$, $\alpha = 0.2$, $\Gamma = 0.001$, $Gr = 3$, $x = 0.2$, $E = 6$ and $\theta = 2.5$ (d); $M = 1.5$, $\beta_1 = 0$, $\alpha = 0.2$, $\Gamma = 0.001$, $Gr = 3$, $x = 0.2$, $E = 6$ and $\theta = 2.5$ (e).

the curves becomes non-linear for $\Gamma \neq 0$. Figs. 3(b)–3(d) depict that pressure rise ΔP_λ increases when values of M, Gr and β_1 are increased.

4.2. Flow characteristics

Fig. 4 illustrates the effects of various parameters on the transverse distributions of longitudinal velocity in a channel. The performed analysis shows that axial velocity at the wall has the same value $u(y = h) = -1$ in the wave frame satisfying the no-slip boundary condition for all values of the parameters. The parametric performance near the channel walls is different when compared with the behavior in the centre of channel. However at the central line of channel $y = 0$ the largest disparity occurs and important results may be listed as follows.

Fig. 4(a) reveals that an increase in Γ causes an increase in the velocity at the centre of channel. Fig. 4(b) shows that M has inverse relation with velocity at the centre of channel. The influence of Grashof number on velocity profile is depicted in Fig. 4(c). This figure elucidates that the velocity is an increasing function of Grashof number. Further an increase in velocity is noticed at the central line $y = 0$ when β_1 increases (Fig. 3(d)).

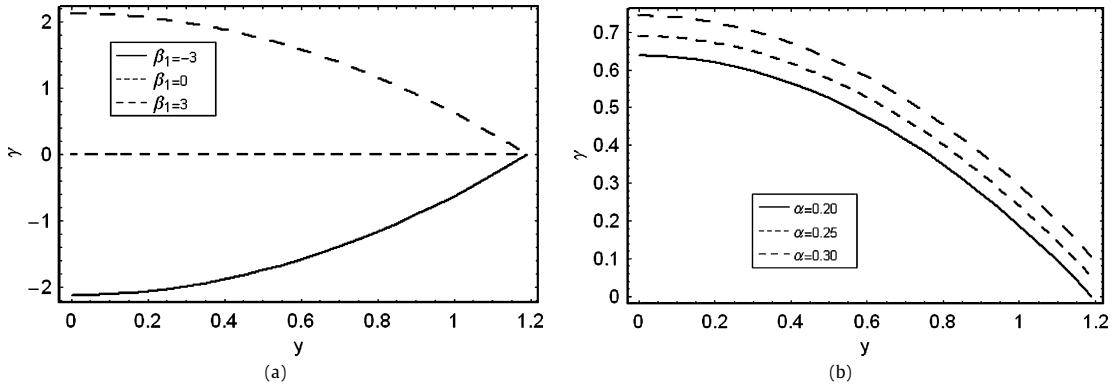

Fig. 7. The temperature distribution γ versus y for $\alpha = 0.2$ and $x = 0.2$ (a); for $\gamma = 0.9$ and $x = 0.2$ (b).

4.3. Magnetic field characteristics

The variation of axial-induced magnetic field h_x and the current density distribution J_z across the channel for various values of Γ, M, Gr, E, R_m and β_1 are displayed in Figs. 5 and 6. The salient extracted results about an axial induced magnetic field are reproduced below.

In the half region of the channel the induced magnetic field is in one direction whereas it is in the opposite direction in the other half region. It is zero at $y = 0$ which is compatible with the boundary condition imposed on magnetic force function.

Figs. 5(a) and 5(b) indicate the variation of axial induced magnetic field h_x against y for the various values of Γ and M. Magnitude of h_x increases when Γ and M increase. Figs. 5(c)–5(e) depict the effects of Gr, β_1 and E on an induced magnetic field h_x versus y. We note that magnitude of h_x decreases when these parameters increase. The influence of magnetic Reynolds number R_m on an axial induced magnetic field h_x is presented in Fig. 4(f). Here magnitude of h_x is an increasing function of R_m.

Fig. 6 serves to present the variation of current density distribution J_z within y for the different values of Γ, M, Gr, E, R_m and β_1. It is noticed that the graphs of current density are parabolic in nature. Increase and decrease in J_z for certain ranges of y show that net current flow is zero. Behavior of parameters at the centre of the channel are quite different from the ones near the walls of channel.

Fig. 6(a) presents the distribution of current density J_z within y for different values of Γ. We noticed that magnitude of J_z decreases when Γ increases at the centre of channel while it increases for certain range of y near the walls of channel. Fig. 6(b) depicts the effect of M on the current density. This shows that magnitude of J_z increases when M is increased at $y = 0$. Fig. 6(c) shows the behavior of J_z against y for the different values Gr. It is evident from the figure that magnitude of J_z decreases when Gr is increased at the centre of channel. Figs. 6(d) and 6(e) reveal that at the centre of channel, the current density J_z presents itself as an decreasing function of β_1 and increasing function of magnetic Reynolds number R_m respectively.

4.4. Temperature characteristics

Fig. 7 is made to analyze the influences of important parameters on the temperature profiles. We noticed that solution corresponding to $\Gamma^{(1)}$ is zero under the employed boundary conditions. Heat sink/source parameter β_1 and amplitude ratio α are the only significant parameters appearing in the temperature distribution. Figs. 7(a) and 7(b) reflect that temperature increases with β_1 and α respectively.

5. Concluding remarks

The peristaltic flow of a fourth grade fluid subjected to heat transfer and induced magnetic field has been examined. The main points of the performed analysis are listed below.

- Both pressure gradient and pressure rise are increasing functions of Γ, M, Gr and β_1.
- The magnitude of velocity is an increasing function of Γ, Gr and β_1 while it decreases at the centre line of the channel when M increases.
- Magnitude of induced magnetic field increases with Γ, M and R_m and decreases with Gr, E and β_1.
- The magnitude of current density profiles has an increasing effect for M and R_m. However, the influence of Gr, β_1 and Γ on the magnitude of current density are opposite to that of M and R_m.
- The temperature distribution is an increasing function of α and β_1.

Acknowledgements

This work has been carried out under the financial support of Higher Education Commission (HEC) of Pakistan. Valuable comments of the referees regarding an earlier version is gratefully acknowledged.

Supplementary material

The Appendix to this Note is supplied as Supplementary material with the electronic version.
Please visit doi:10.1016/j.crme.2010.06.004.

References

[1] Abd El Hakeem Abd El Naby, A.E.M. El Misery, M.F. Abd El Kareem, Effects of magnetic field on trapping field through peristaltic motion for generalized Newtonian fluid in a channel, Physica A 367 (2006) 79–92.
[2] T. Hayat, A. Afsar, M. Khan, S. Asghar, Peristaltic transport of a third order fluid under the effect of a magnetic field, Comput. Math. Applications 53 (2007) 1074–1087.
[3] T. Hayat, N. Ali, Effects of an endoscope on the peristaltic flow of a micropolar fluid, Math. Comput. Modelling 48 (2008) 721–733.
[4] T. Hayat, M.U. Qureshi, N. Ali, The influence of slip on the peristaltic motion of a third order fluid in an asymmetric channel, Phys. Lett. A 372 (2008) 2653–2664.
[5] S. Srinivas, M. Kothandapani, The influence of heat and mass transfer on MHD peristaltic flow through a porous space with compliant walls, Appl. Math. Comput. 213 (2009) 197–208.
[6] T. Hayat, Q. Hussain, N. Ali, Influence of partial slip on the peristaltic flow in a porous medium, Phys. Lett. A 387 (2008) 3399–3409.
[7] M.H. Haroun, Effect of Deborah number and phase difference on peristaltic transport of a third-order fluid in an asymmetric channel, Math. Comput. Modelling 12 (2007) 1464–1480.
[8] M.H. Haroun, Non-linear peristaltic flow of a fourth grade fluid in an inclined asymmetric channel, Comput. Mater. Sci. 39 (2007) 333.
[9] M. Kothandapani, S. Srinivas, Peristaltic transport of a Jeffrey fluid under the effect of magnetic field in an asymmetric channel, Int. J. Non-Linear Mech. 43 (2008) 915–924.
[10] D. Tripathi, S.K. Pandey, S. Das, Peristaltic flow of viscoelastic fluid with fractional Maxwell model through a channel, Appl. Math. Comput. 215 (2010) 3645–3654.
[11] S. Srinivas, M. Kothandapani, The influence of heat and mass transfer on MHD peristaltic flow through a porous space with compliant walls, Appl. Math. Comput. 213 (2009) 197–208.
[12] T. Hayat, S. Hina, N. Ali, Simultaneous effects of slip and heat transfer on the peristaltic flow, Comm. Nonlinear Sci. Numer. Simul. 15 (2010) 1526–1537.
[13] T. Hayat, Y. Wang, K. Hutter, S. Asghar, A.M. Siddiqui, Peristaltic transport of an Oldroyd-B fluid in a planar channel, Mathematical Problems in Engineering 4 (2004) 347–376.
[14] T. Hayat, N. Ahmad, N. Ali, Effects of an endoscope and magnetic field on the peristalsis involving Jeffrey fluid, Comm. Nonlinear Sci. Numer. Simul. 13 (2008) 1581–1591.
[15] N.T.M. Eldabe, M.F. Al-Sayad, A.Y. Galy, H.M. Sayed, Peristaltically induced motion of a MHD biviscosity fluid in a non-uniform tube, Physica A 383 (2007) 253–266.
[16] T.W. Latham, Fluid Motion in a Peristaltic Pump, MIT, Cambridge MA, 1966.
[17] Kh.S. Mekheimer, Effect of induced magnetic field on peristaltic flow of a couple stress fluid, Phys. Lett. A 372 (2008) 4271–4278.
[18] Kh.S. Mekheimer, Peristaltic flow of a magneto-micropolar fluid: Effect of induced magnetic field, J. Appl. Math., doi:10.1155/2008/570825.
[19] T. Hayat, Y. Khan, N. Ali, Kh.S. Mekheimer, Effect of an induced magnetic field on the peristaltic flow of a third order fluid, Numer. Methods Partial Diff. Eqs. 26 (2010) 345–360.
[20] Kh.S. Mekheimer, Y.A. Elmaboud, The influence of heat transfer and magnetic field on peristaltic transport of a Newtonian fluid in a vertical annulus: Application of an endoscope, Phys. Lett. A 372 (2008) 1657–1665.
[21] S. Srinivas, R. Gayathri, Peristaltic transport of a Newtonian fluid in a vertical asymmetric channel with heat transfer and porous medium, Appl. Math. Comput. 215 (2009) 185–196.
[22] S. Srinivas, M. Kothandapani, Peristaltic transport in an asymmetric channel with heat transfer – A note, Int. Comm. Heat Mass Transfer 35 (2008) 514–522.
[23] S. Nadeem, T. Hayat, N.S. Akbar, M.Y. Malik, On the influence of heat transfer in peristalsis with variable viscosity, Int. J. Heat Mass Transfer 52 (2009) 4722–4730.
[24] T. Hayat, M.U. Qureshi, Q. Hussain, Effect of heat transfer on the peristaltic flow of an electrically conducting fluid in a porous space, Appl. Math. Mod. 33 (2009) 1862–1873.
[25] Kh.S. Mekheimer, S.Z.A. Husseny, Y. Abd Elmaboud, Effects of heat transfer and space porosity on peristaltic flow in a vertical asymmetric channel, Numer. Methods Partial Diff. Eqs. 26 (2010) 747–770.
[26] S. Nadeem, N.S. Akbar, Effects of heat transfer on the peristaltic transport of MHD Newtonian fluid with variable viscosity: Application of Adomian decomposition method, Comm. Nonlinear Sci. Numer. Simul. 14 (2009) 3844–3855.